AN ABSTRACT OF THE THESIS OF

Tyler P. Montgomery for the degree of Honors Baccalaureate of Science in Biology presented on February 27, 2013. Title: Bioethanol production from lignocellulosic biomass: assessing genes linked to acetic acid stress in *Saccharomyces cerevisiae*.

Abstract approved:

_____

Alan T. Bakalinsky

Lignocellulosic biomass represents a vast and renewable source of fermentable sugar for production of biofuels. However, native lignocellulose—comprised of cellulose, hemicellulose and lignin—is refractory to degradation because the crystalline cellulose is not easily hydrolyzed by cellulases. Standard chemical treatments of lignocellulose to reduce the crystallinity of cellulose prior to enzymatic hydrolysis also generate fermentation inhibitors, including acetic and other organic acids, furfural, hydroxymethyl furfural, and phenolic compounds. To increase the acetic acid resistance of one of the major microorganisms used to ferment lignocellulose-derived sugars, mutations in three genes were introduced and evaluated in a prototrophic laboratory strain of *Saccharomyces cerevisiae,* S288c, and were introduced into the industrial strain D5A. Previous work had shown that loss of *FPS1*, encoding an acetic acid channel, and loss of *EDE1* and *MVB12*, encoding proteins involved in endocytosis, increased acetic acid resistance. Disruption of *FPS1* in S288c resulted in somewhat greater resistance at low concentrations (80-120 mM acetic acid) but not at concentrations greater than 120 mM. Combined genetic and molecular analyses of the disruptions of *FPS1, EDE1* and *MVB12* in D5A indicated that D5A was diploid, and that only one of the two alleles of each of these genes had been deleted.

Key Words: lignocellulosic biomass, ethanol, acetic acid, yeast, *Saccharomyces cerevisiae,* S288c, D5A, Fps1, Ede1, Mvb12

Corresponding e-mail address: montgoty@onid.orst.edu

Bioethanol production from lignocellulosic biomass:

assessing genes linked to acetic acid stress in *Saccharomyces cerevisiae*

by

Tyler P. Montgomery

A PROJECT

Submitted to

Oregon State University

University Honors College

In partial fulfillment of
The requirements for the
degree of

Honors Baccalaureate of Science in Biology (Honors Associate)

Presented February 27, 2013
Commencement June 2013

Honors Baccalaureate of Science in Biology project of Tyler P. Montgomery presented on February 27, 2013.

APPROVED:

Mentor, representing Food Science & Technology

Committee Member, representing Food Science & Technology

Committee Member, representing Botany & Plant Pathology

Department Head, Food Science & Technology

Dean, University Honors College

I understand that my project will become part of the permanent collection of Oregon State University, University Honors College. My signature below authorizes release of my project to any reader upon request.

Tyler P. Montgomery, Author

Acknowledgements

First and foremost, I would like to thank Dr. Alan Bakalinsky, Associate Professor of Food Science and Technology, for mentoring me throughout this endeavor. For almost two years, Dr. Bakalinsky has helped me through the thesis process, investing valuable time in me and the research I conducted. Without his guidance and access to his laboratory, this thesis would not have been possible.

I would also like to thank Ph.D. candidate Jun Ding, who works in Dr. Bakalinsky's laboratory. She taught me many of the experimental techniques used for this thesis and also helped troubleshoot experimental problems when they arose. Many times, when Dr. Bakalinsky was unavailable, Jun was the first person I would run to. Jun's help and oversight were integral in the completion of experimental work.

Former and current undergraduate assistants Jan Bierma, Virginia Usher and Garrett Holzwarth were an invaluable resource in the laboratory. They helped troubleshoot experimental problems and helped me refine experimental techniques.

I would also like to thank committee members Dr. Mike Penner, Associate Professor of Food Science and Technology, and Dr. Jeff Chang, Associate Professor of Botany and Plant Pathology. Their participation in my defense and recommendations on how to improve my thesis were greatly appreciated.

USDA-NIFA is acknowledged for support of the research presented in this thesis.

Table of Contents

List of Figures

List of Tables

List of Appendix Figures

List of Appendix Tables

Introduction

Physical description of lignocellulosic biomass

Lignocellulosic biomass (LCB), the main constituent of plant cell walls, is comprised of cellulose, hemicellulose, and lignin (Figure 1) (Rubin, 2008). Cellulose is made of unbranched chains of hydrogen-bonded glucose molecules arranged in a crystalline-like structure (Saha, 2004). Hemicellulose is a heterogeneous mixture of branched pentoses (e.g., xylose, arabinose) and hexoses (e.g., mannose, glucose, galactose) (Saha, 2004). Lignin is a three-dimensional polymer of phenylpropanoid units that hold cellulose and hemicellulose together by cross-linking with hemicellulose (Rubin, 2008). Their relative proportions vary based on the source material, but LCB usually contains 35-50% cellulose, 20-35% hemicellulose and 10-25% lignin (Saha, 2004; Rubin, 2008).

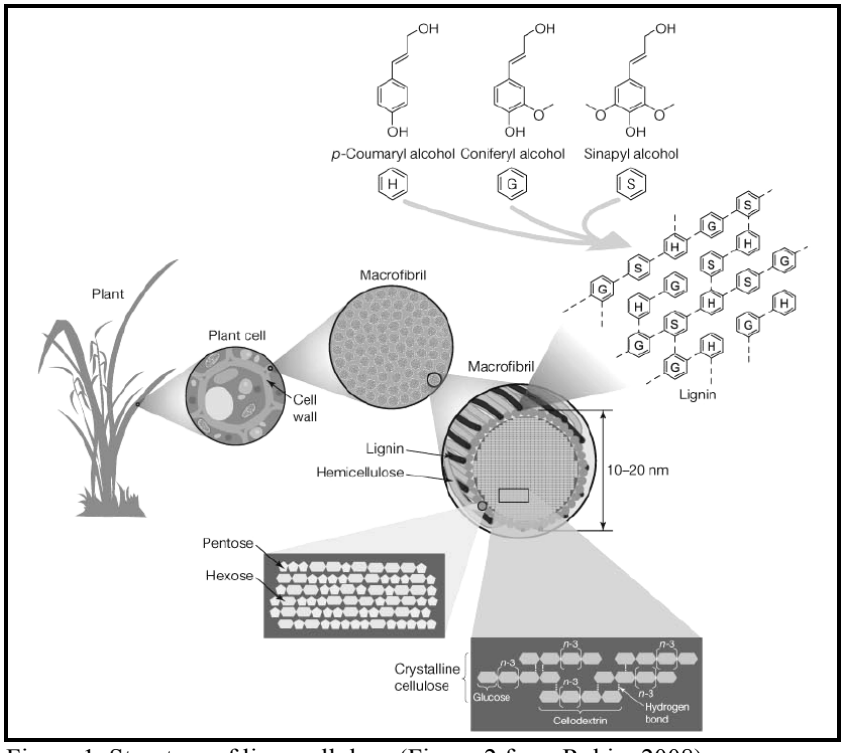

Figure 1. Structure of lignocellulose (Figure 2 from Rubin, 2008)

Utilizing lignocellulosic biomass

There is great interest in exploiting LCB as a renewable source of fermentable sugars in the form of cellulose and hemicellulose, which can be used to generate ethanol and other biofuels. However, native LCB is highly resistant to degradation, referred to as recalcitrance (Akin, 2007). The recalcitrance is due to the lignification of plant fibers and the crystalline structure of cellulose (Himmel et al, 2007). Recalcitrance can be reduced by treatment with high-pressure steam, high-pressure liquid ammonia, lime, or dilute sulfuric acid (Saha, 2004). Dilute acid treatment reduces the recalcitrance of LCB by reducing the crystallinity of cellulose and opening up its structure (Agbor et al., 2011). Hemicellulose and lignin are solubilized and extracted into the liquid fraction. A disadvantage of dilute acid and other treatments, however, is the generation of fermentation inhibitors, compounds derived from the partial breakdown of cellulose, hemicellulose and lignin into phenolic compounds, furan derivatives, and weak acids (Figure 2; Palmqvist & Hahn-Hägerdal, 2000). Acetic acid is specifically generated from the hydrolysis of acetylated hemicellulose during dilute acid and other treatments of LCB (Saha, 2004).

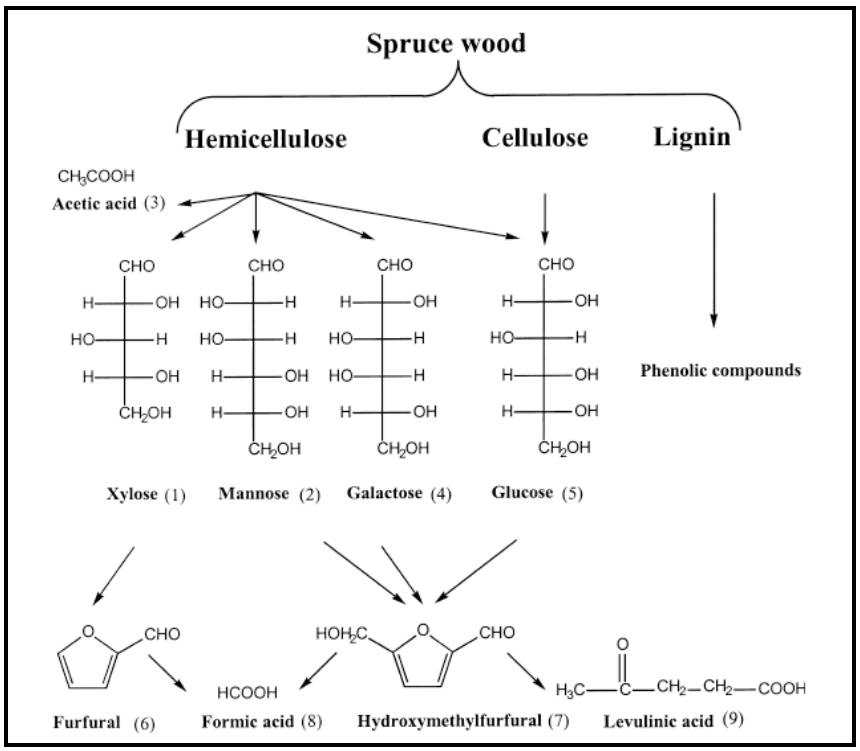

Figure 2. By-products from the pretreatment of LCB with dilute acid (Figure 1 from Palmqvist & Hahn-Hägerdal, 2000).

Weak acids are problematic because they can inhibit microbial growth and decrease ethanol production (Narendranath et al., 2001). The undissociated acids are largely taken up by passive diffusion and then dissociate inside the cytosol, lowering intracellular pH, reducing enzymatic function (Palmqvust & Hahn-Hägerdal, 2000; Verduyn et al., 1992), and possibly causing additional stress.

Acid resistance in *Saccharomyces cerevisiae*

Mollapour and Piper (2007) found that in addition to uptake via passive diffusion, acetic acid is taken up by yeast through the aquaglyceroporin Fps1, which was previously described as a glycerol channel (Luyten et al., 1995). Disruption of *FPS1* significantly

lowered intracellular acetate levels and conferred acetic acid resistance in a laboratory strain of yeast.

Research by Ph.D. candidate Jun Ding has suggested involvement of the endocytic pathway proteins Ede1 and Mvb12 in acetic acid resistance (Ding et al., 2013). Ede1 and Mvb12 are involved in transporting ubiquitinated membrane proteins to the lysosome for degradation (Oestrich et al, 2007; Swanson et al., 2006). She proposes that an impaired endocytic pathway, lacking Mvb12 or Ede1, prolongs retention of nutrient transporters, increasing nutrient uptake in the presence of acetic acid which has been shown to inhibit amino acid uptake (Bauer et al, 2003; Hueso et al., 2012) and uptake of other nutrients as well (Ding et al., 2013). Mutants lacking *EDE1* or *MVB12* were found to be more resistant to acetic acid than wild-type cells (Ding et al., 2013).

Acid resistance in the Acetic Acid Bacteria

The acetic acid bacteria (AAB) are a group of organisms that can grow in the presence of very high concentrations of acetic acid, ~6 % (v/v) for *Acetobacter* (Krisch & Szajáni, 1997). Comparatively, the model organism *Escherichia coli* is affected by as little as 0.1% (v/v) (Diez-Gonzalez and Russell, 1997). Understanding the way AAB survive the low pH conditions could further acid resistance work in *Saccharomyces cerevisiae.* Three different mechanisms that confer acetic acid resistance in the acetic acid bacteria have been described. Specifically, resistance has been ascribed to 1) a modified citric acid cycle (Mullins et al., 2008), 2) a proton:acetic acid antiporter (Matsushita et al., 2005), and 3) a putative ABC transporter for acetic acid (Nakano et al., 2006).

A modified citric acid cycle (CAC) was found in *Acetobacter aceti* that provides an alternative route for acetyl-CoA synthesis that requires no ATP and which consumes

acetic acid directly (Mullins et al., 2008). This modified CAC contains an enzyme encoded by AarC that has succinyl-CoA:acetate-CoA transferase activity (SCACT). SCACT converts acetic acid and succinyl-CoA to acetyl CoA and succinate, respectively. Acetyl-CoA is normally produced from acetic acid and CoA by ATP-dependent acetyl-CoA synthetase.

A proton:acetic acid antiporter was found in *Acetobacter aceti* (Matsushita et al., 2005). This antiporter exports acetic acid produced internally. Coupled with the movement of acetic acid is the import of protons. Upon addition of respiratory substrates, inside-out vesicles containing the transporter were found to accumulate high levels of acetic acid. The authors concluded that the transporter relies on a proton motive force.

A putative ABC transporter responsible for the export of intracellular acetic acid has also been described in *Acetobacter aceti* (Nakano et al., 2006). The membrane protein aatA was found to contain amino acid sequences characteristic of an ATP Binding Cassette (ABC) protein family, which uses the energy of ATP to actively transport its substrate. While the transport of acetic acid was not directly assayed, the authors concluded that the increased levels of extracellular acetic acid produced by mutants overexpressing aatA was evidence of aatA being an ABC transporter.

Focus of this thesis

This thesis focused on analyzing the effect of mutations previously identified in auxotrophic laboratory strains of *Saccharomyces cerevisiae* that increased acetic acid resistance (Ding et al., 2013; Mollapour and Piper, 2007). Specifically, I determined whether mutations in *FPS1, EDE1,* and *MVB12* could increase acetic acid resistance in previously untested prototrophic strains of *Saccharomyces cerevisiae*. Genes were disrupted with a kanamycin-resistance cassette (KanMX) and the constructed mutants were then subjected to dose-response analysis at a range of acetic acid concentrations. Growth (A_{600}) of the mutants was compared to that of wild-type cells. I hypothesized that *FPS1*Δ, *EDE1*Δ and *MVB12*Δ mutants in the S288c and D5A genetic backgrounds would be more resistant to acetic acid than either parent.

Materials & Methods

Yeast strains

Saccharomyces cerevisiae S288c, a prototrophic strain, (*MAT*α *SUC2 gal2 mal mel flo1 flo8-1 hap1 ho bio1 bio6*), D5A (ATCC 200062), an industrial strain used for ethanol production, and auxotrophic BY4742 (*MATα his3 leu2 lys2 ura3*) and *FPS1*, *EDE1*, and *MVB12* deletion mutants in the BY4742 background were used in this study.

Mutant construction

To determine the effect of deleting *FPS1, EDE1* and *MVB12* on acetic acid resistance in previously untested strains, these genes were disrupted in D5A and S288c by replacing the wild-type alleles with PCR-generated deletion alleles harboring the KanMX cassette flanked by sequences homologous to the upstream and downstream regions of the respective genes. These alleles were obtained from the respective *FPS1*Δ*::KanMX, EDE1*Δ*::KanMX,* and *MVB12*Δ*::KanMX* disruption strains in the BY4742-based deletion library (Winzeler et al., 1999). The S288c and D5A strains were then transformed individually with the linear PCR fragments to facilitate homologous recombination which was expected to result in replacement of the wild-type alleles with the disrupted copies. Transformants were selected by plating on rich medium, YEPD, containing the kanamycin analog, G418.

PCR

Primers to generate *FPS1, EDE1* and *MVB12* deletion alleles and to confirm integration were designed using genomic sequences obtained from the Saccharomyces Genome Database (Yeastgenome.org) and created using PrimerBLAST software (PubMed.org), Table 1. The KanC primer which anneals to the middle of the KanMX sequence was used with appropriate downstream primers for each deleted gene to confirm the presence of KanMX at target loci.

Table 1. Primers used to generate gene disruption fragments and to confirm mutants.

$Ede1_{DisUp}$:	5'-CACAATCATTACCCGTCGGCGCT-3'
$Ede1_{DisLo}$:	5'-ACAAGGACGATCCTGGAAAAGGGT-3'
$Fps1_{up}$:	5'-ATTGCCCGGCCCTTTTTGCG-3'
$Fps1_{lo}$:	5'-GGTGACCAGGCTGAGTTCATGTCA-3'
KanC :	5'-TGATTTTGATGACGAGCGTAAT-3'
$Mvb12_{DisUp}$:	5'-ACCGTTCAGAGGCTGTCCGAGA-3'
$Mvb12_{DisLo}$:	5'-CCGCGTTACGTAGGACTGCCC-3'

The PCR program used for deletion allele construction and genotypic confirmation is listed in Table 2.

Table 2. PCR program

Step	Temperature (ºC)	Duration (min:sec)	No. of Cycles
Initial Denature	94	3:00	1
Denature	94	0:15	35
Annealing*	58-62*	0:30	
Extension	68	10:00	
Final Extension	68	10:00	1

*The annealing temperature selected was based on primer Tm values in order to optimize strand-pairing.

Yeast transformation

Strains were transformed as described (Gietz & Woods, 2002), with the following modifications:

1. 'Day 1' overnight cultures were inoculated into 1 ml of 2X YEPD (1% yeast extract, 2% peptone, 2% glucose), not the prescribed 5 ml.
2. 'Day 2' cell titer was determined by counting cells in a haemocytometer, with 10 µl of a 1:50 cell suspension placed on the slide. Budding cells were counted as individual cells (i.e., a cell with two buds was counted as 3 cells).
3. Thirty ml of pre-warmed 2X YEPD was used instead of the prescribed 50 ml, and was inoculated with X µl of the overnight culture to achieve a cell concentration of 5×10^6 cells/ml.
4. Step 7: cells were resuspended in X µl of water to maintain 2×10^9 cells/ml, instead of the prescribed 1.0 ml of water.
5. Step 9: about 1 µg of linear DNA and 400 ng of plasmid DNA were used per transformation.
6. Step 13: transformed cells were re-suspended by light mixing with a pipette in 2X YEPD, instead of the prescribed water. Cells were not vortexed because too vigorous mixing has been found to reduce transformation efficiencies.
7. Step 14: transformed cells were re-suspended in 2X YEPD and placed on a 200 rpm shaker at 30°C for 60 minutes, before being plated on YEPD + G418 selection plates. Allowing the transformants to 'recover' on 2X YEPD before being plated with the antibiotic G418 greatly increased transformation efficiency.

Confirmation of Transformants

Mutants were confirmed by phenotype and independently by genotype:

1. Phenotypic confirmation: Colonies on transformation plates were streaked onto fresh YEPD + G418 plates and allowed to grow for 48 hours at 30°C, or until isolated colonies appeared. The appearance of isolated colonies constituted phenotypic confirmation of the presence of an integrated KanMX construct.
2. Genotypic confirmation: Isolated colonies found on the phenotypic confirmation plates were then tested genotypically by diagnostic PCR and gel electrophoresis. Mutants were deemed genotypically confirmed if the observed PCR fragments corresponded to the expected sizes of the disrupted alleles.

When a putative mutant was confirmed both phenotypically and genotypically, it was then prepared for long-term storage by suspending an overnight YEPD culture in YEPD + 20% glycerol and transferring it to -70º C. Working cultures were maintained on YEPD + G418 selection plates at 4º C

Dose response analysis

Resistance to acetic acid was tested using a growth protocol described in Ding et al., (2013). The protocol allows for the quantitative analysis of relative growth at increasing concentrations of acetic acid. Relative growth, assessed as A_{600} values, is the growth observed in the presence of a given concentration of acetic acid, divided by growth in the absence of acetic acid, multiplied by 100. One mL yeast cultures grown in YNB-4.8, a synthetic minimal medium at pH 4.8, were inoculated with mutant and parental control strains and incubated at 30°C at 200 RPM for 24 hours. Cells were collected by centrifugation, washed twice with sterile water**,** and re-suspended in 1.0 ml of sterile water to serve as an inoculum. YNB-4.8 containing 0, 80, 120, 160, 200, 220 and 240 mM acetic acid were inoculated with X µl of the cell suspension to obtain ~ 2 x 10^5 cells/ml in a final volume of 1 mL, in triplicate. Stocks of 10X YNB-4.8 and 2N acetic acid, pH 4.8 were used. A_{600} values were measured after 48 h at 30°C and 200 RPM. Samples were diluted as needed so that A_{600} readings did not exceed 0.3 (the linear range of the spectophotometer for turbid solutions). Values were then multiplied by the dilution factor to calculate the actual A_{600} readings.

Results

S288c FPS1Δ::KanMX

In order to construct S288c FPS1Δ::KanMX, PCR primers were designed to amplify the deletion allele of *FPS1* present in the BY4742 FPS1Δ strain from the Yeast Deletion Project. S288c was transformed with the resulting FPS1Δ::KanMX PCR fragment. Transformants were selected on YEPD + G418 plates.

Phenotypic confirmation was performed by re-streaking putative transformants on YEPD + G418 plates (Figure 3). Wild-type S288c cells and BY4742 FPS1Δ::KanMX cells were streaked as negative and positive controls, respectively. S288c grew on YEPD but not on YEPD + G418, as expected. BY4742 FPS1Δ::KanMX grew on both YEPD and YEPD + G418, as expected. The putative S288c FPS1Δ::KanMX mutant grew on both YEPD and YEPD + G418, confirming the presence of KanMX.

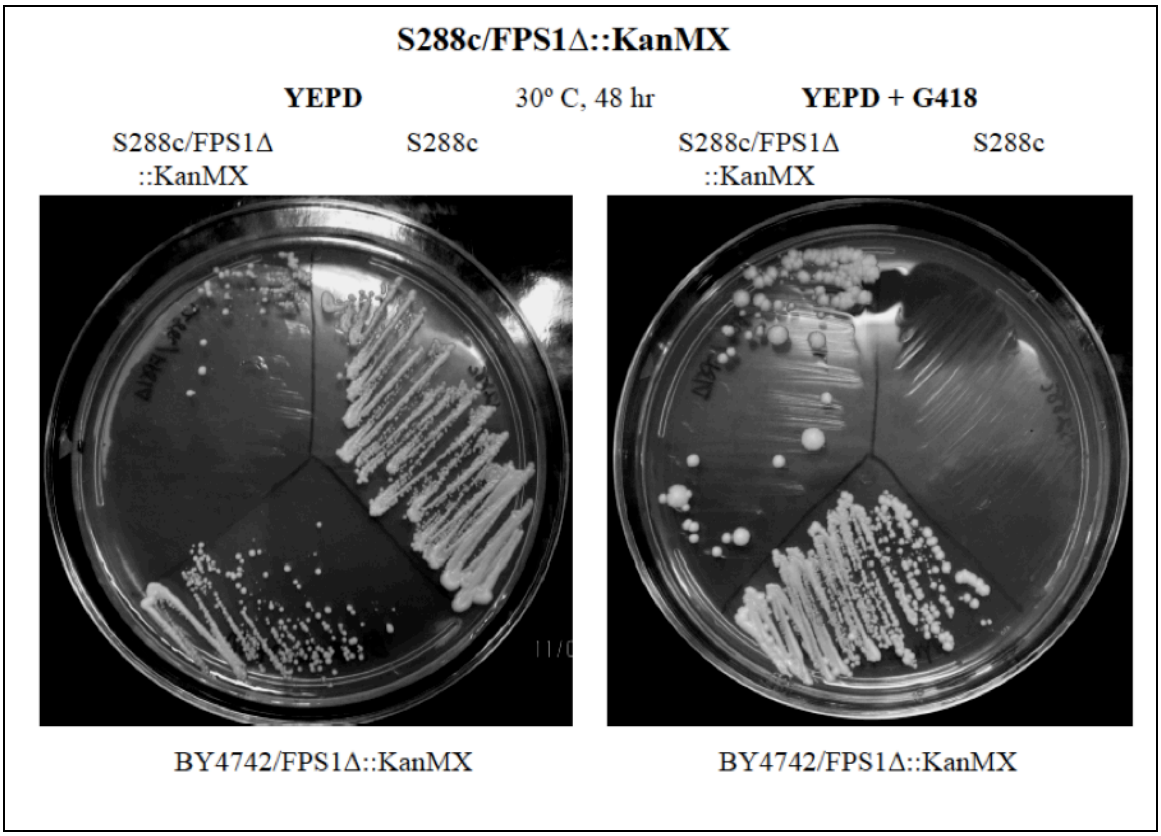

Figure 3. Phenotypic confirmation of S288c FPS1Δ::KanMX. S288c, S288c FPS1Δ and BY4742 FPS1Δ cultures were streaked for isolated colonies on YEPD and YEPD + G418 plates. The negative control, S288c, grew on YEPD but not YEPD + G418, as expected. The positive control, BY4742 FPS1Δ::KanMX, grew on both YEPD and YEPD + G418, as expected. The putative mutant, S288c FPS1Δ::KanMX, grew on both YEPD and YEPD + G418, phenotypically confirming the presence of the kanamycin resistance cassette within the mutant.

Genotypic confirmation was performed using PCR primers to amplify *FPS1* and a fragment only possible if KanMX were present within the disrupted *FPS1* ORF. Expected and observed data are listed in Table 3. Gel electrophoretic results are shown in Figure 4.

Table 3. Expected/observed results from the genotypic confirmation of S288c FPS1Δ::KanMX

Strain	Lane	Primers	Expected fragment	Observed fragment
S288c	**4**	Fps1up/Fps1Lo	2,427 bp	~2,400 bp
	5	KanC/Fps1Lo	-	-
S288c FPS1Δ::KanMX	**2**	Fps1up/Fps1Lo	2,037 bp	~2,000 bp
	3	KanC/Fps1Lo	844 bp	~850 bp

Lanes 1 and 6 are a DNA ladder (fragment sizes are indicated in base pairs). Lanes 2 and 3 show the *FPS1*Δ allele in the constructed mutant, S288c FPS1Δ. Lane 2 shows the expected band of ~2,000 basepairs, generated using FPS1up and FPS1lo primers, confirming disruption of the *FPS1* ORF. Lane 3 shows a band of ~850 basepairs using the internal primer KanC and FPS1lo, confirming the presence of KanMX at the *FPS1* ORF. KanC is a primer which anneals to an internal sequence within the kanamycin cassette. A fragment should only be present if *FPS1* had been disrupted with KanMX. Lanes 4 and 5 show the wild-type *FPS1* allele from the parent, S288c. Lane 4 shows wild-type *FPS1*, ~2,400 basepairs, with primers FPS1up and FPS1lo. Lane 5 shows no band, using the internal primer KanC and FPS1Lo, confirming the lack of KanMX at the *FPS1* ORF within this parent strain.

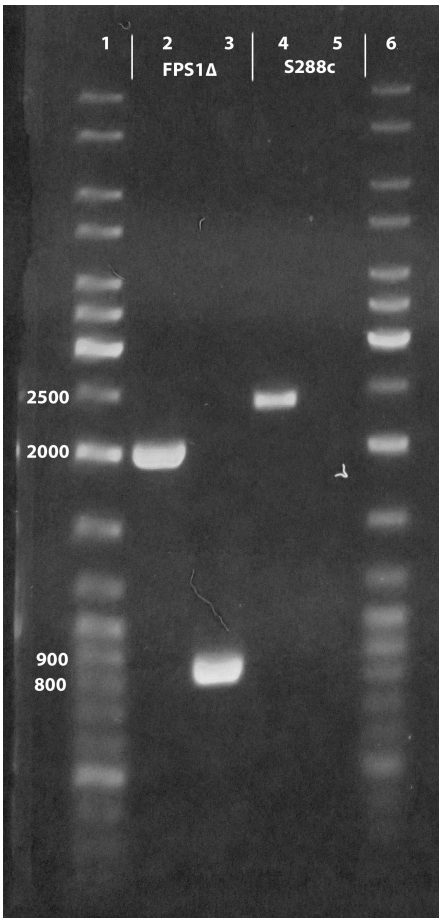

Figure 4. Gel electrophoresis results for S288c FPS1Δ::KanMX.

The phenotypic and genotypic analyses indicate that the *FPS1* allele in S288c was disrupted by the KanMX cassette.

D5A FPS1Δ::KanMX

In order to construct D5A FPS1Δ::KanMX, the same PCR primers used to amplify the FPS1Δ::KanMX allele from BY4742 FPS1Δ were used. D5A was transformed with the resulting FPS1Δ::KanMX PCR fragment and transformants were selected on YEPD + G418 selection plates.

Phenotypic confirmation was performed by re-streaking putative transformants on YEPD + G418 (Figure 5). Wild-type D5A cells and BY4742 FPS1Δ::KanMX cells were also streaked for isolated colonies as negative and positive controls, respectively. D5A grew on YEPD but not YEPD + G418, as expected. BY4742 FPS1Δ::KanMX grew on both YEPD and YEPD + G418, as expected. The putative D5A FPS1Δ::KanMX mutant grew on both YEPD and YEPD + G418, confirming the presence of KanMX.

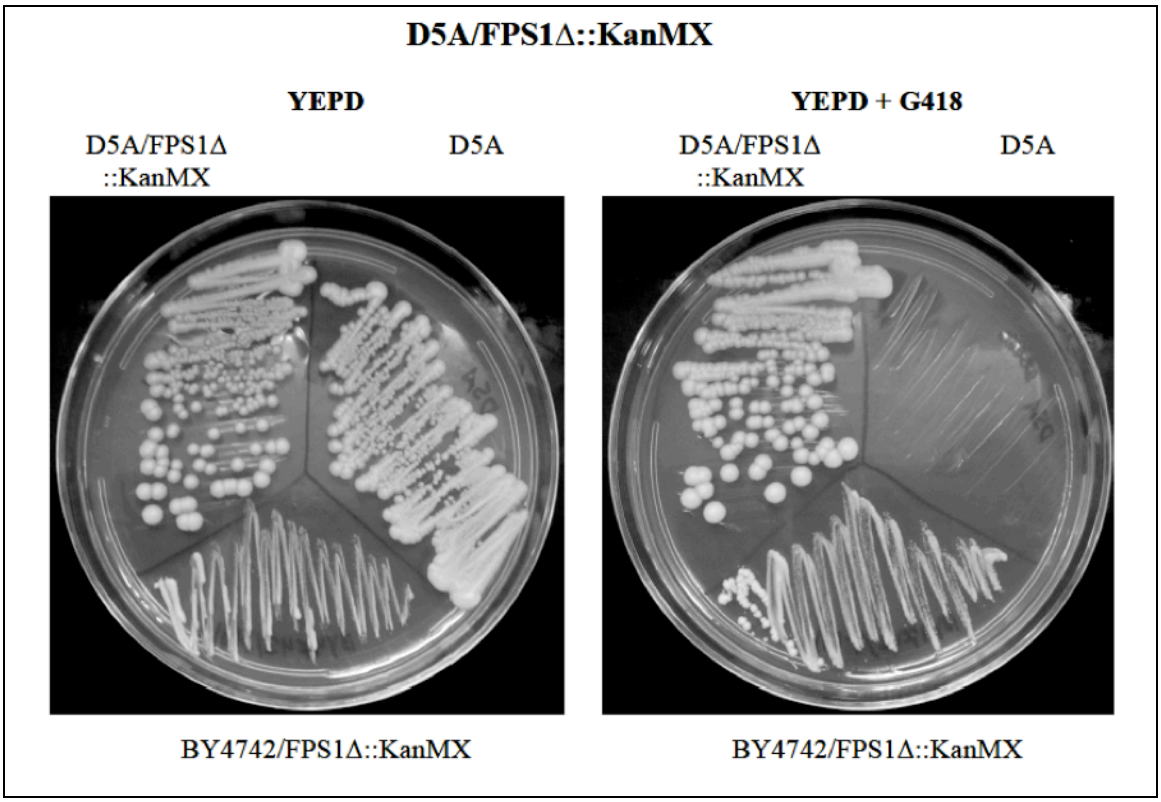

Figure 5. Phenotypic confirmation of D5A FPS1Δ::KanMX. D5A, D5A FPS1Δ and BY4742 FPS1Δ cultures were streaked for isolated colonies on YEPD and YEPD + G418 plates. The negative control, D5A, grew on YEPD but not YEPD + G418, as expected. The positive control, BY4742 FPS1Δ::KanMX, grew on both YEPD and YEPD + G418, as expected. The putative mutant, D5A FPS1Δ::KanMX, grew on both YEPD and YEPD + G418, phenotypically confirming the presence of the Kanamycin resistance cassette within the mutant.

Genotypic confirmation was performed using PCR primers to amplify the *FPS1* ORF and a fragment only possible if KanMX were present at the *FPS1* ORF. Expected and observed data are listed in Table 4. Gel electrophoretic results are shown in Figure 5.

Table 4. Expected/observed results from the genotypic confirmation of D5A FPS1Δ::KanMX.

Strain	Lane	Primers	Expected fragment	Observed fragment
D5A	**2**	Fps1up/Fps1Lo	2,427 bp	~2,400 bp
	3	KanC/Fps1Lo	-	-
D5A FPS1Δ::KanMX	**4**	Fps1up/Fps1Lo	2,037 bp	~2,400 & ~2,000 bp
	5	KanC/Fps1Lo	844 bp	~850 bp

Lanes 1 and 6 are a DNA ladder. Lanes 2 and 3 show the wild-type *FPS1* allele from the parent, D5A. Lane 2 shows a band of ~2,400 base pairs, the wild-type *FPS1 ORF*. Lane 3 shows no band using the internal primer KanC and FPS1lo, confirming the lack of KanMX in the parent. Lanes 4 and 5 show the *FPS1*Δ allele in the constructed mutant, D5A FPS1Δ. Lane 4 shows two bands of ~2,000 basepairs and ~2,500 basepairs, which is indicative of D5A having two copies of *FPS1*. One is disrupted with KanMX (~2,000 bp) and the other is wild-type (~2,500 bp). Lane 5 shows a band of ~850 basepairs with primers KanC and FPS1lo, confirming the presence of KanMX at the *FPS1* ORF.

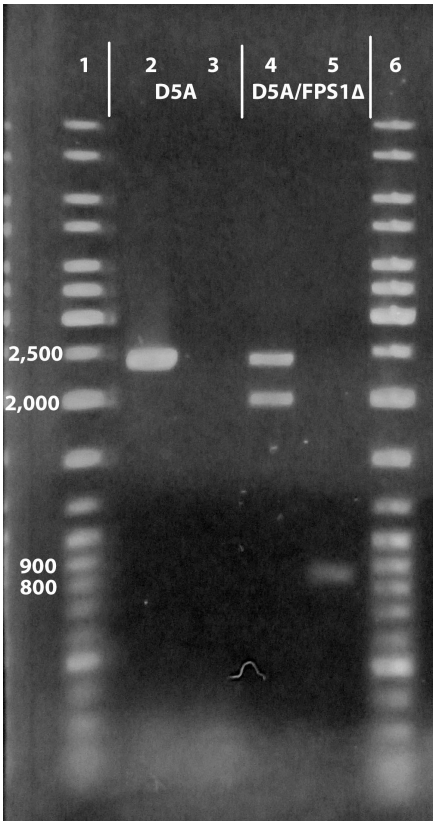

Figure 6. Gel electrophoresis results for D5A FPS1Δ::KanMX. The two bands in lane 4 indicate that only one copy of the *FPS1* ORF was disrupted in the diploid D5A.

Based on the results of the phenotypic and genotypic analyses of the putative D5A FPS1Δ::KanMX mutant, only one out of two copies of the *FPS1* ORF was disrupted.

D5A EDE1Δ::KanMX

In order to construct D5A EDE1Δ::KanMX, PCR primers designed by Jun Ding to amplify the deletion allele of *EDE1* in BY4742 EDE1Δ::KanMX were used. D5A was transformed with the resulting EDE1Δ::KanMX PCR fragment. Transformants were selected on YEPD + G418 selection plates.

Phenotypic confirmation was performed by re-streaking putative transformants on YEPD + G418 (Figure 7). Wild-type D5A cells and BY4742 EDE1Δ::KanMX cells were also streaked for isolated colonies as negative and positive controls, respectively. D5A grew on YEPD but not YEPD + G418, as expected. BY4742 EDE1Δ::KanMX grew on both YEPD and YEPD + G418, as expected. The putative D5A EDE1Δ::KanMX mutant grew on both YEPD and YEPD + G418, confirming the presence of KanMX.

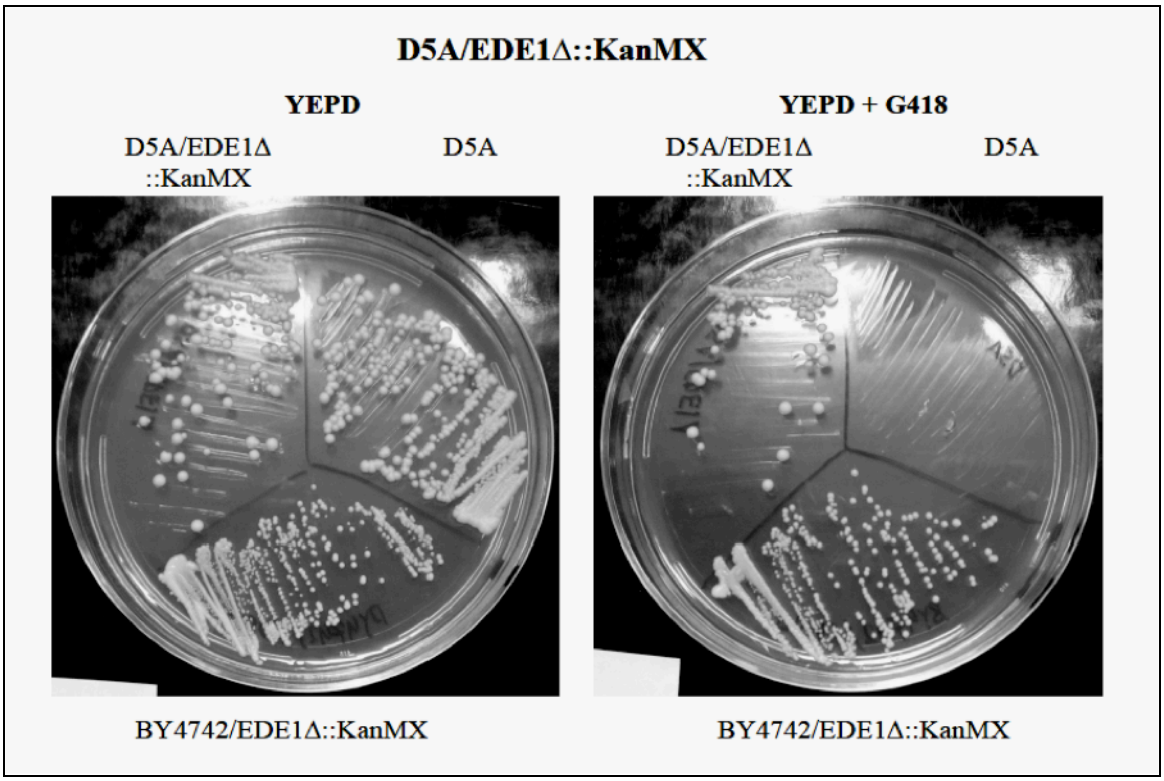

Figure 7. Phenotypic confirmation of D5A EDE1Δ::KanMX. D5A, D5A EDE1Δ and BY4742 EDE1Δ cultures were streaked for isolated colonies on YEPD and YEPD + G418 plates. The negative control, D5A, grew on YEPD but not YEPD + G418, as expected. The positive control, BY4742 EDE1Δ::KanMX, grew on both YEPD and YEPD + G418, as expected. The putative mutant, D5A EDE1Δ::KanMX, grew on both YEPD and YEPD + G418, phenotypically confirming the presence of the Kanamycin resistance cassette within the mutant.

Genotypic confirmation was performed by using PCR primers to amplify the *EDE1* ORF and a fragment only amplifiable if KanMX were present at the *EDE1* ORF. Expected and observed data are listed in Table 5. Gel electrophoretic results are shown in Figure 8.

Table 5. Expected/observed results from the genotypic confirmation of D5A EDE1Δ::KanMX.

Strain	Lane	Primers	Expected fragment	Observed fragment
D5A	**2**	Ede1DisUp/ Ede1DisLo	4,504 bp	~4,500 bp
	3	KanC/Ede1DisLo	-	-
D5A EDE1Δ::KanMX	**4**	Ede1DisUp/ Ede1DisLo	2,053 bp	~4,500 & ~2,000 bp
	5	KanC/Ede1DisLo	715 bp	~750 bp

Lanes 1 and 6 are a DNA ladder. Lanes 2 and 3 show the wild-type *EDE1* allele in the parent, D5A. Lane 2 shows the expected wild-type ORF band of ~4,500 basepairs. Lane 3 shows no band, confirming the lack of KanMX at the *EDE1* ORF. Lanes 4 and 5 show the *FPS1*Δ allele from the constructed mutant, D5A EDE1Δ. Lane 4 shows a result similar to the D5A FPS1Δ mutant, which is consistent with D5A having two copies of the *EDE1* ORF. Lane 5 shows the expected band of ~750 basepairs, confirming the presence of KanMX at one *EDE1* locus.

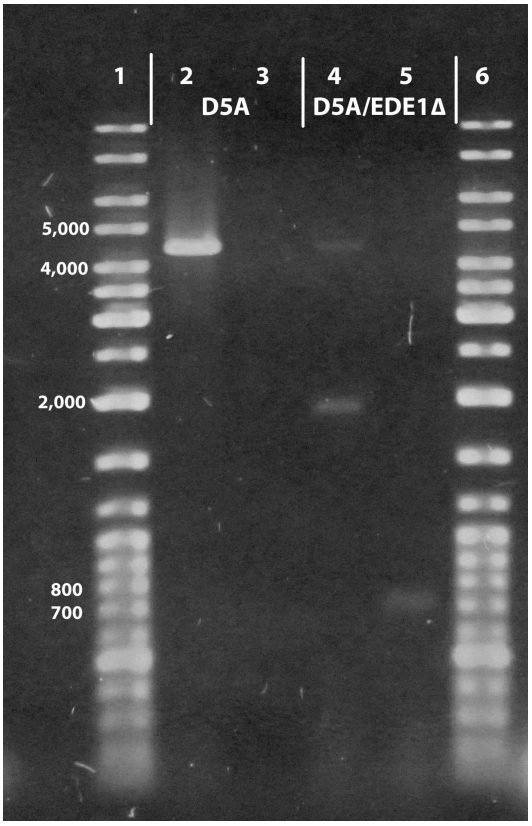

Figure 8. Gel electrophoresis results for D5A EDE1Δ::KanMX. The two bands in lane 4 indicate that only one copy of the *EDE1* ORF was disrupted in the diploid D5A.

Based on the results of the phenotypic and genotypic analyses of the putative D5A EDE1Δ::KanMX mutant, only one out of two copies of the *EDE1* ORF was disrupted.

D5A MVB12Δ::KanMX

In order to construct D5A MVB12::KanMX, PCR primers designed by Jun Ding to amplify the deletion allele of *MVB12* in BY4742 MVB12Δ::KanMX, were used. D5A was transformed with the resulting MVB12Δ::KanMX PCR fragment. Resulting transformants were selected on YEPD + G418 selection plates.

Phenotypic confirmation was performed by re-streaking putative transformants on YEPD + G418 (Figure 9). Wild-type D5A cells and BY4742 MVB12Δ::KanMX cells were also streaked for isolated colonies as negative and positive controls, respectively. D5A grew on YEPD but not YEPD + G418, as expected. BY4742 MVB12Δ::KanMX grew on both YEPD and YEPD + G418, as expected. The putative D5A MVB12Δ::KanMX mutant grew on both YEPD and YEPD + G418, confirming the presence of KanMX.

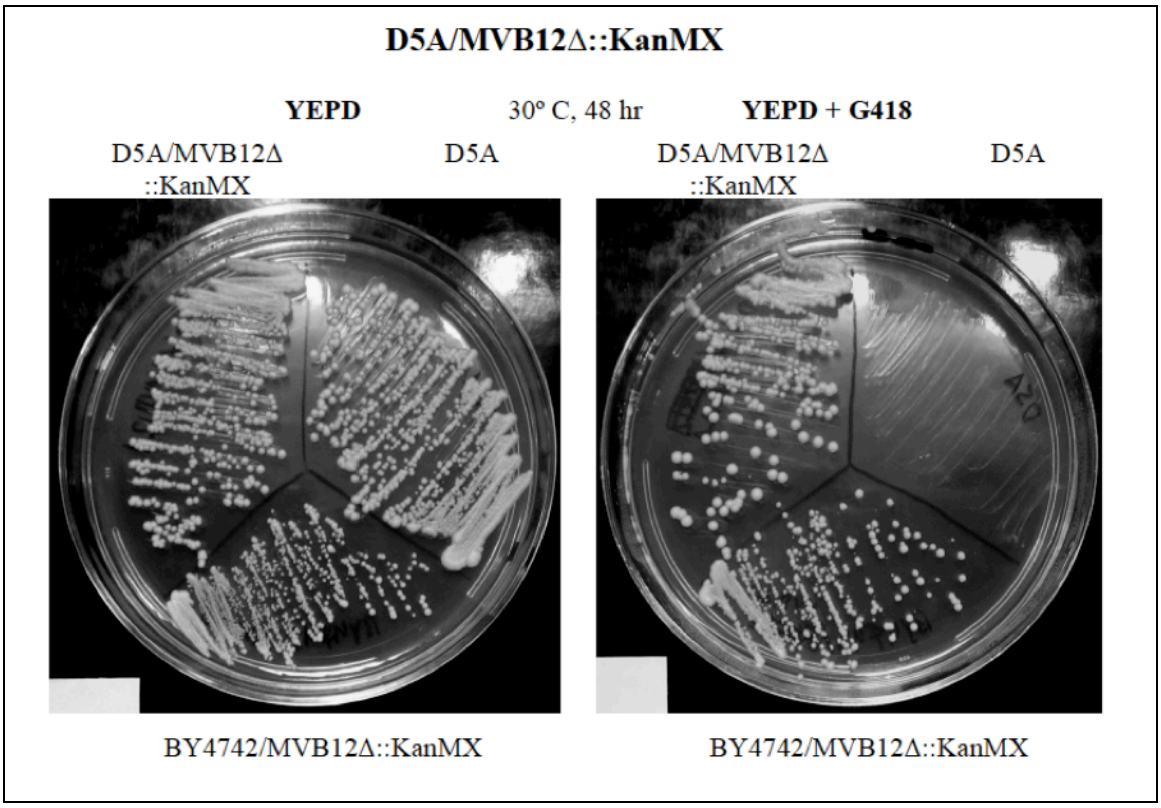

Figure 9. Phenotypic confirmation of D5A MVB12Δ::KanMX. D5A, D5A MVB12Δ and BY4742 MVB12Δ cultures were streaked for isolated colonies on YEPD and YEPD + G418 plates. The negative control, D5A, grew on YEPD but not YEPD + G418, as expected. The positive control, BY4742 MVB12Δ::KanMX, grew on both YEPD and YEPD + G418, as expected. The putative mutant, D5A MVB12Δ::KanMX, grew on both YEPD and YEPD + G418, phenotypically confirming the presence of the Kanamycin resistance cassette within the mutant.

Genotypic confirmation was performed by using PCR primers to amplify the *MVB12* ORF and a fragment only amplifiable if KanMX were present at the *MVB12* ORF. Expected and observed data are listed in Table 6. Gel electrophoretic results are shown in Figure 10.

Table 6. Expected/observed results from the genotypic confirmation of D5A MVB12Δ::KanMX.

Strain	Lane	Primers	Expected fragment	Observed fragment
D5A	**2**	Mvb12DisUp / Mvb12DisLo	724 bp	~750 bp
	3	KanC / Mvb12DisLo	-	-
D5A MVB12Δ ::KanMX	**4**	Mvb12DisUp / Mvb12DisLo	2,053 bp	~2,000 bp
	5	KanC / Mvb12DisLo	944 bp	~950 bp

Lanes 1 and 6 are a DNA ladder. Lanes 2 and 3 show the wild-type *MVB12* ORF in the parent, D5A, and confirm the presence of the wild-type *MVB12* ORF and the lack of KanMX. Lanes 4 and 5 contain the *MVB12*Δ allele from the constructed mutant D5A MVB12Δ, and show the same result as discussed previously for the *FPS1*Δ and *EDE1*Δ mutants. While KanMX is present at the *MVB12* ORF, only one allele was disrupted.

Based on the results of the phenotypic and genotypic analyses of the putative D5A MVB12Δ::KanMX mutant, only one of two copies of *MVB12* was disrupted.

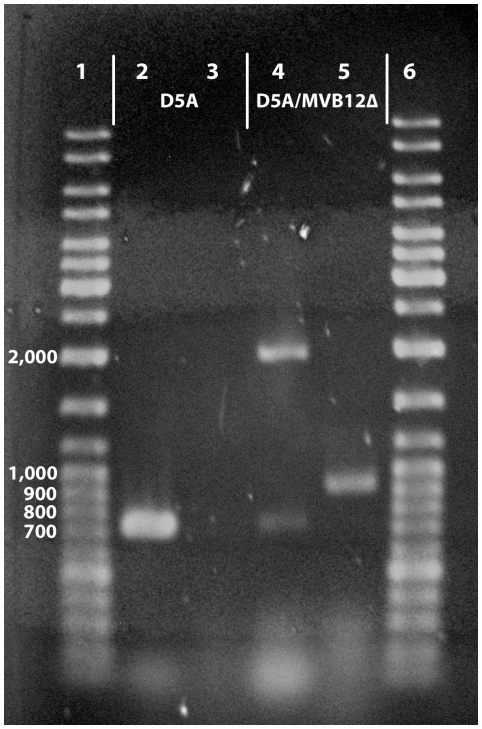

Figure 10. Gel electrophoresis results for D5A MVB12Δ::KanMX. The two bands in lane 4 indicate that only one copy of the *MVB12* ORF was disrupted in the diploid D5A.

Is D5A diploid?

Because physical evidence was obtained suggesting that D5A was diploid, a genetic analysis was undertaken to confirm this possibility (A. Bakalinsky, data not shown, 2012). Briefly, the physical evidence was the presence of both wild-type and mutant alleles of *FPS1* (chromosome XII), *EDE1* (chromosome II), and *MVB12* (chromosome VII) in the constructs that had been transformed with the Kan-based disruption alleles.

D5A had been obtained from the American Type Culture Collection (ATCC) as strain 200062, originally isolated from cheese whey and provided to the collection by T. K. Hayward. In our hands, this strain was able to mate as a MAT alpha strain and failed to sporulate, which is indicative of being haploid. A subsequent literature search uncovered an earlier report (Bailey et al., 1982) suggesting that the strain was a diploid, monosomic for chromosome III which carries the mating type locus. Based solely on the ability to mate and sporulate, it is not possible to distinguish a diploid, monosomic for chromosome III, from a diploid that is homozygous at the MAT locus. To determine whether the strain was a diploid homozygous for the *MAT alpha* allele which would allow it to mate and prevent it from sporulating, or was a diploid monosomic for chromosome III, crosses were carried out between genetically-marked haploid strains and two of the constructed strains D5A *FPS1*Δ*::KanMX/FPS1* and D5A *EDE1*Δ*::KanMX/EDE1*. Segregation analysis for the input markers performed on the spore progeny was consistent with D5A being diploid and not monosomic for chromosome III (A. Bakalinsky, data not shown, 2012).

Dose response analysis

S288c and S288c FPS1Δ::KanMX were subjected to dose response analysis. Dose response data for S288c and S288c FPS1Δ are represented graphically (Figure 11) and in Table 7. Raw data are listed in the Appendix. Dose response data for the D5A disruptants are in the Appendix, as these strains still carry undisrupted copies of either *FPS1, EDE1* or *MVB12.*

Dose response data were graphed to compare growth between S288c and S288c FPS1Δ in the presence of acetic acid (Figure 11). Four replicates were performed. The mean relative growth was plotted as a function of acetic acid concentration. Error bars are the standard errors of the mean. At lower concentrations of acetic acid (<140 mM) *FPS1*Δ grew better than the wild-type. A significant difference in growth was measured at 80 mM acetic acid (Figure 11). However, wild-type S288c grew better at higher concentrations of acetic acid (>140 mM). A significant difference in growth was also measured at 220 mM acetic acid where the wild-type parent performed better than the *FPS1*Δ mutant (Figure 11).

A summary of the S288c and S288c FPS1Δ dose response data is listed in table 9, by replicate. The IC_{50} value is the concentration of acetic acid at which growth was 50% of growth in the absence of acetic acid. A_{600} (no acetic acid) values are mean values at 0 mM acetic acid. MIC (minimum inibitory concentration) values are the concentrations of acetic acid which prevented visible growth.

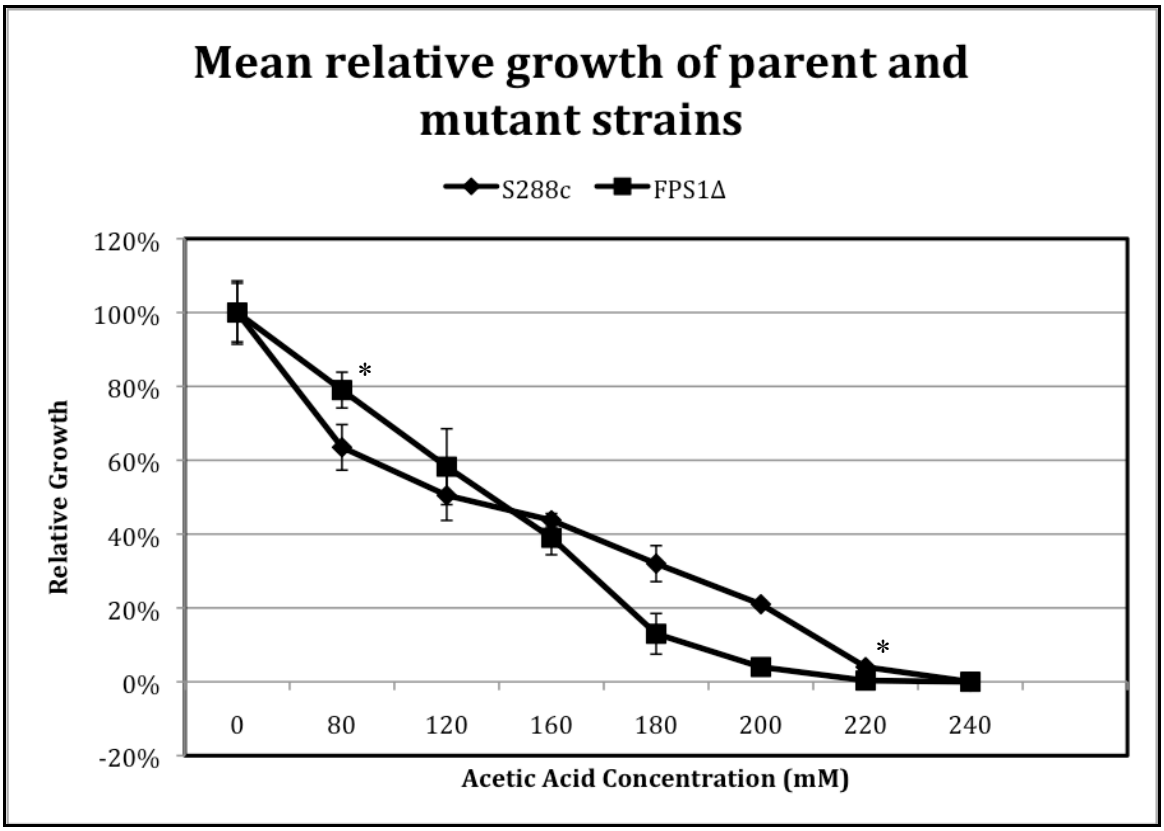

Figure 11. Mean relative growth of S288c and S288c FPS1Δ::KanMX (n=4). The Y-axis is relative growth which represents the A_{600} ratio of growth in the presence of acetic acid to growth in the absence of acetic acid. Error bars are standard errors of the mean. An asterisk indicates a significant difference in growth ($p<0.05$, Student's two-sided T-Test). At 80 mM acetic acid, *FPS1*Δ exhibited significantly greater growth, whereas wild-type S288c grew significantly better at 220 mM acetic acid, albeit slightly.

Replicate	S288c			S288c FPS1Δ		
	IC_{50}	MIC	A_{600} (no acetic acid)	IC_{50}	MIC	A_{600}
1	126 mM	220 mM	5.1	111 mM	200 mM	4.9
2	98 mM	220 mM	4.5	128 mM	180 mM	4.3
3	142 mM	240 mM	3.9	143 mM	220 mM	3.2
4	118 mM	240 mM	4.7	170 mM	240 mM	4.1
Mean	**121.00 mM**	**230.00 mM**	**4.55**	**138.00 mM**	**210.00 mM**	**4.13**
Std. Dev.	18.29 mM	11.55 mM	0.50	25.02 mM	25.82 mM	0.70
RSD	15.12%	5.02%	10.99%	18.13%	12.30%	17.07%

Table 7. Summary of dose response experiments. The IC_{50} value refers to the concentration of acetic acid which reduced growth by 50%. The A_{600} value refers to the OD value of cells in 0 mM acetic acid. The MIC value (minimum inhibitory concentration value) refers to the concentration of acetic acid which halted all growth.

S288c A_{600} values in 0 mM acetic acid ranged from 3.9 to 5.1, ± 0.50. FPS1Δ cultures ranged from 3.2 to 4.9, ± 0.70 (Table 7). Parent cultures had slightly higher A_{600} values than FPS1Δ cultures but these differences were not significant.

The concentration of acetic acid which reduced growth to 50 % (IC_{50}) was 121±18 mM for S288c, and 138±25 mM for FPS1Δ (Table 7). While FPS1Δ cultures had a higher mean IC_{50} value compared to S288c, there was no significant difference between S288c and FPS1Δ IC_{50} values.

The concentration of acetic acid which halted all cellular growth (MIC) was 230±12 mM for S288c, and 210±26 mM for FPS1Δ (Table 7). S288c cultures, overall, had a higher mean MIC concentration than FPS1Δ but there was no significant difference between the minimum inhibitory concentration for S288c and FPS1Δ.

Discussion

The data presented in this thesis suggest that disruption of *FPS1* does not affect acetic acid resistance in prototrophic *Saccharomyces cerevisiae* S288c. This result contrasts with the findings of Mollapour and Piper (2007) and Zhang et al. (2011).

Mollapour and Piper (2007) compared acetic acid resistance of BY4741, a multiply-auxotrophic haploid, with an otherwise isogenic strain missing *FPS1*. Resistance was assessed visually as growth on a YEPD plate, pH 4.5 containing acetic acid. Inocula consisted of cells grown overnight in YEPD, pH 4.5 that were then diluted to an A_{600} value of 0.5 prior to spotting 5 µl aliquots of 10-fold dilutions onto test plates containing 0, 100, 120 or 140 mM acetic acid. Growth was scored after 3 days at 30° C,

Figure 12. By this assay, the *FPS1* deletion strain in the auxotrophic BY4741 genetic background was able to grow in the presence of up to 140 mM acetic acid, whereas the wild-type parent stopped growing at concentrations greater than 100 mM.

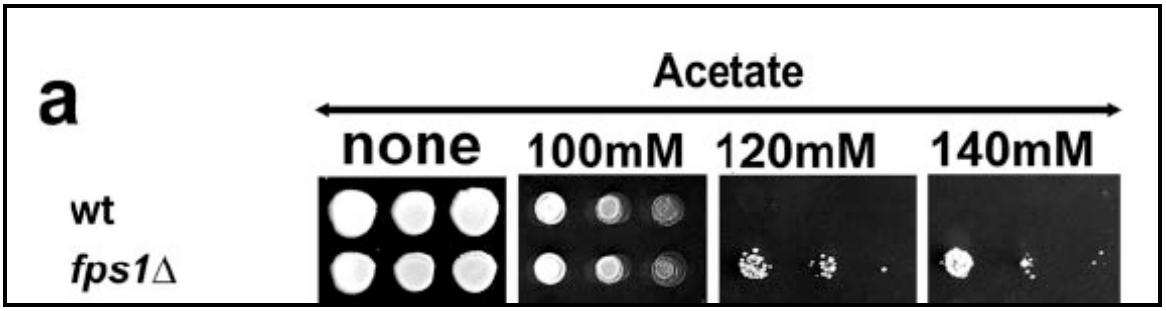

Figure 12. Figure 1a from Mollapour and Piper (2007) showing growth for wild-type and FPS1Δ cultures (a 1:10 dilution series grown [3 days, 30°C] on pH 4.5 YEPD agar containing the indicated level of acetic acid).

While Mollapour and Piper (2007) observed a difference in growth between wild-type and FPS1Δ cultures at 120 and 140 mM acetic acid, I saw no difference in growth between prototrophic S288c and an *FPS1*Δ mutant in the S288c genetic background at concentrations as high as 220 mM acetic acid (Figures 11 & 12). However, passive diffusion of undissociated acetic acid at 220 mM acetic acid is likely to be so great as to negate loss of the Fps1 channel.

Zhang et al. (2011) compared the growth of CE25, an industrial ethanol production strain of unknown origin, with an isogenic *FPS1*Δ mutant disrupted with the *CUP1* gene. Acetic acid tolerance was analyzed on plates following growth of both cultures in 5 mL YEPD at 28º C and 150 rpm for 16 h. Washed cells were re-suspended in 1 mL of sterile water and kept at room temperature for 2 h before a loopful of the serially diluted suspensions were placed on plates containing 0, 70, 78, 87, or 104 mM acetic acid (Figure 13). Unlike Mollapour and Piper (2007) who stated that equal

numbers of cells were plated per strain, it was unclear whether the starting number of cells in the two cultures were identical.

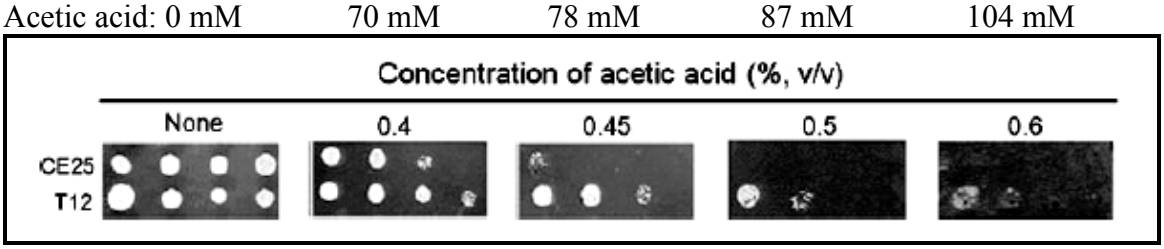

Figure 13. Figure 3 from Zhang et al. (2010). Growth of wild-type (CE25) and the *FPS1*Δ mutant (T12).

Zhang et al. (2011) found that the *FPS1*Δ culture grew better than wild-type in as little as 70 mM and as great as 104 mM acetic acid (Figure 13). However, at 104 mM acetic acid, even the *FPS1*Δ mutant appeared to grow poorly.

While both Mollapour and Piper (2007) and Zhang et al. (2010) demonstrated a difference in acetic acid tolerance between wild-type and *FPS1*Δ cultures, the wild-type strains failed to grow at 120 mM and 87 mM acetic acid, respectively. I found one significant difference in growth measured at 80 mM acetic acid ($p<0.05$, two-tailed Student's T-Test), within the range of concentrations tested by Mollapour and Piper (2007) and Zhang et al. (2010). At 80 mM acetic acid, the S288c *FPS1*Δ mutant exhibited significantly better relative growth than the parent (Figure 11), consistent with the possibility that disruption of the *FPS1* allele confers resistance at low concentrations. In contrast, the wild-type S288c culture I tested exhibited 20% relative growth at a concentration of 220 mM acetic acid. At this high concentration, most acetic acid may be entering the cell by passive diffusion, rather than through the Fps1 channel. If correct, loss of the Fps1 channel would likely have little effect on growth at this high

concentration. At 220 mM acetic acid, S288c exhibited very poor growth but significantly better than the *FPS1*Δ mutant (Figure 11, Student's two-tailed T-Test).

Repeated attempts to disrupt *FPS1, EDE1,* and *MVB12* in D5A resulted in loss of only one of two copies of each gene. While the mutants were able to grow on selective plates, diagnostic PCR analysis showed the presence of both wild-type and disrupted alleles. On-going work in the laboratory to disrupt the second alleles is based on introduction of a hygromycin B resistance cassette, which will permit selection of the resistant transformants that are already resistant to kanamycin.

Conclusions

The important findings of this study are two-fold. First, in a prototrophic background at a relatively high concentration of acetic acid (>150 mM), loss of *FPS1* did not increase resistance to acetic acid in *S. cerevisiae*. This is important because it indicates the limits of acetic acid resistance conferred by this mutation. However, loss of *FPS1* increased resistance at lower concentrations of acetic acid (<120 mM) mirrored in previous studies (Mollapour and Piper, 2007; Zhang et al., 2011).

Second, the industrial yeast D5A that has been used as a standard strain in previous studies of renewable bioenergy, appears to be an unusual diploid, homozygous for the *MAT alpha* allele. This is important because disruptions of genes in this strain that may confer increased resistance to acetic acid will require assuring that both copies are targeted.

Works Cited

Agbor, V. B., Cicek, N., Sparling, R., Berlin, A., & Levin, D. B. (2011). Biomass pretreatment: fundamentals toward application. *Biotechnology Advances, 29*, 675-685.

Akin, D. E. (2007). Grass lignocellulose: strategies to overcome recalcitrance. *Applied Biochemistry & Biotechnology, 137*, 3-15.

Andrés-Barrao, C., Saad, M.M., Chappius, M.L., Boffa, M., Perret, X., Pérez, R.O., Barja, F. (2012). Proteome analysis of Acetobacter pasteurianus during acetic acid fermentation. *Journal of Proteomics*, 75, 1701-1717.

Bailey, R.B., Benitez, T., Woodward, A. (1982). Saccharomyces cerevisiae mutants resistant to catabolite repression: use in cheese whey hydrolysate fermentation. *Applied and Environmental Microbiology, 44*, 631-639.

Bauer, B. E., Rossington, D., Mollapour, M., Mamnun, Y., Kuchler, K., & Piper, P. W. (2003). Weak organic acid stress inhibits aromatic amino acid uptake by yeast, causing a strong influence of amino acid auxotrophies on the phenotypes of membrane transporter mutants. *European Journal of Biochemistry, 270*, 3189-3195.

Diez-Gonzalez, F., Russell, J.B. (1997). The ability of Escherichia coli O157:H7 to decrease its intracellular pH and resist the toxiticy of acetic acid. *Microbiology*, *143,* 1175-1180.

Ding, J., Bierma, J., Smith, M.R., Poliner, E., Wolfe, C., Hadduck, A.N., Zara, S., Jirikovic, M., van Zee, K., Penner, M.H., Patton-Vogt, J., Bakalinsky, A.T. (2013). Acetic Acid Inhibits Nutrient Uptake in *Saccharomyces cerevisiae*. In review.

Faga, B. A., Wilkins, M. R., & Banat, I. M. (2010). Ethanol production through simultaneous saccharification and fermentation of switchgrass using Saccharomyces cerevisiae D5A and thermotolerant *Kluyveromyces marxianus* IMB strains. *Bioresource Technology, 101*, 2273-2279.

Fukaya, M., Takemura, H., Tayama, K., Okumura, H., Kawamura, Y., Horinouchi, S., et al. (1993). The aarC gene responsible for acetic acid assimilation confers acetic acid resistance on acetobacter aceti. *Journal of Fermentation and Bioengineering, 76*, 270-275.

Gietz, R., & Woods, R. (2002). Transformation of yeast by the Liac/SS carrier DNA/PEG method. In C. Guthrie, & G. R. Fink, *Methods in Enzymology: Guide to Yeast Genetics and Molecular and Cell Biology - Part B* (Vol. 350, pp. 87-96). San Diego: Academic Press.

Himmel, M. E., Ding, S.-Y., Johnson, D. K., Adney, W. S., Nimlos, M. R., Brady, J. W., et al. (2007). Biomass recalcitrance: engineering plants and enzymes for biofuels production. *Science, 315*, 804-807.

Hueso G, Aparicio-Sanchis R, Montesinos C, Lorenz S, Murguía JR, Serrano R. (2012). A novel role for protein kinase Gcn2 in yeast tolerance to intracellular acid stress. *Journal of Biochemistry, 441*, 255-264.

Krisch, J., Szajáni, B. (1997). Ethanol and acetic acid tolerance in free and immobilized cells of Saccharomyces cerevisiae and Acetobacter aceti. *Biotechnology Letters, 19*, 525-528.

Luyten, K., Albertyn, J., Skibbe, W. F., Prior, B. A., Ramos, J., Thevelein, J. M., et al. (1995). Fps1, a yeast member of the MIP family of channel proteins, is a facilitator for glycerol uptake and efflux and is inactive under osmotic stress. *The EMBO Journal, 14*, 1360-1371.

Matsushita, K., Inoue, T., Adachi, O., & Toyama, H. (2005). *Acetobacter aceti* possesses a proton motive force-dependent efflux system for acetic acid. *Journal of Bacteriology, 187*, 4346-4352.

Mollapour, M., & Piper, P. W. (2007). Hog1 mitogen-activated protein kinase phosphorylation targets the yeast fps1 aquaglyceroporin for endocytosis, thereby rendering cells resistant to acetic acid. *Molecular and Cellular Biology, 27*, 6446-6456.

Mullins, E. A., Francois, J. A., & Kappock, T. J. (2008). A specialized citric acid cycle requiring succinyl-coenzyme A (CoA):acetate CoA-transferase (AarC) confers acetic acid resistance on the acidophile Acetobacter aceti. *Journal of Bacteriology, 190*, 4933-4940.

Nakano, S., Fukaya, M., & Horinouchi, S. (2006). Putative ABC transporter responsible for acetic acid resistance in acetobacter aceti. *Applied and Environmental Microbiology, 72*, 497-505.

Narendranath, N., Thomas, K., & Ingledew, W. (2001). Effects of acetic acid and lactic acid on the growth of Saccharomyces cerevisiae in a minimal medium. *Journal of Industrial Microbiology & Biotechnology, 26*, 171-177.

Oestrich, A. J., Davies, B. A., Payne, J. A., & Katzmnn, D. J. (2007). Mvb12 is a novel member of ESCRT-I involved in cargo selection by the multivesicular body pathway. *Molecular Biology of the Cell, 18*, 646-657.

Palmqvist, E., & Hahn-Hägerdal, B. (2000). Fermentation of lignocellulosic hydrolysates. II: inhibitors and mechanisms of inhibition. *Bioresource Technology, 74*, 25-33.

Rubin, E. M. (2008). Genomics of cellulosic biofuels. *Nature, 454*, 841-845.

Saha, B. C. (2004). Lignocellulose biodegradation and applications in biotechnology. In B. C. Saha, & K. Hayashi, *Lignocellulose Biodegradation* (1-34). Washington: Oxford University Press.

Suryawati, L., Wilkins, M. R., Bellmer, D. D., Huhnke, R. L., Maness, N. O., & Banat, I. M. (2008). Simultaneous saccharification and fermentation of kanlow switchgrass pretreated by hydrothermolysis using *Kluyveromyces marxianus* IMB4. *Biotechnology and Bioengineering, 101*, 894-902.

Swanson, K. A., Hicke, L., & Radhakrishnan, I. (2006). Structural basis for monoubiquitin recognition by the Ede1 UBA domain. *Journal of Molecular Biology, 358*, 713-724.

Verduyn, C., Postma, E., Scheäers, W.A., Dijken, J.P. (1992). Effect of benzoic acid on metabolic fluxes in yeasts: a continous-culture study on the regulation of respiration and alcoholic fermentation. *Yeast* 8, 501-517.

Winzeler, Elizabeth A., Daniel D. Shoemaker, Anna Astromoff, Hong Liang, Keith Anderson, Bruno Andre, Rhonda Bangham, Rocio Benito, Jef D. Boeke, Howard Bussey, Angela M. Chu, Carla Connelly, Karen Davis, Fred Dietrich, Sally Whelen Dow, Mohamed El Bakkoury, Francoise Foury, Stephen H. Friend, Erik Gentalen, Guri Giaever, Johannes H. Hegemann, Ted Jones, Michael Laub, Hong Liao, Nicole Liebundguth, David J. Lockhart, Anca Lucau-Danila, Marc Lussier, Nasiha M'Rabet, Patrice Menard, Michael Mittmann," Chai Pai, Corinne Rebischung, Jose L. Revuelta, Linda Riles, Christopher J. Roberts, Petra Ross-MacDonald, Bart Scherens, Michael Snyder, Sharon Sookhai-Mahadeo, Reginald K. Storms, Steeve Veronneau, Marleen Voet, Guido Volckaert, Teresa R. Ward, Robert Wysocki, Grace S. Yen,' Kexin yu, Katja Zimmermann, Peter Philippsen, Mark Johnston, Ronald W. Davis (1999). Functional characterization of the S. cerevisiae genome by gene deletion and parallel analysis. *Science*, *285,* 901-906.

Zhang, J.-G., Liu, Z.-Y., He, Z.-P., Guo, Z.-N., Lu, Y., & Zhang, B.-r. (2011). Improvement of acetic acid tolerance and fermentation performance of Saccharomyces cerevisiae by disruption of the FPS1 aquaglyceroporin gene. *Biotechnology Letters, 33*, 277-284.

Appendix

Table A1. S288c Raw dose response data

S288c acetic acid exposure YNB-4.8 adjusted data							
Replicate 1		**Actual A_{600}***					
Acetic Acid (mM)	**A**	**B**	**C**	**Mean**	**Std. Dev.**	**% of Control**	**RSD**
0	5.096	5.154	5.022	5.091	0.0662	100%	1.30%
80	3.244	3.002	-	3.123	0.1711	61%	5.48%
120	2.976	2.452	-	2.714	0.3705	53%	13.65%
140	2.18	2.198	-	2.189	0.0127	43%	0.58%
160	2.238	2.587	-	2.413	0.2468	47%	10.23%
200	2.078	2.117	-	2.098	0.0276	41%	1.31%
220	0.259	0.28	-	0.269	0.0145	5%	5.38%
Replicate 2		**Actual A_{600}**					
Acetic Acid (mM)	**A**	**B**	**C**	**Mean**	**Std. Dev.**	**% of Control**	**RSD**
0	5.152	4.532	3.77	4.485	0.6922	100%	15.44%
80	2.435	2.26	2.511	2.402	0.1287	54%	5.36%
120	2.268	2.109	1.737	2.038	0.2725	45%	13.37%
160	1.379	1.555	1.58	1.505	0.1095	34%	7.28%
180	0.635	0.843	1.032	0.836	0.1983	19%	23.71%
200	0.182	0.152	0.148	0.161	0.0186	4%	11.60%
220	0.068	0.012	0.024	0.035	0.0296	1%	85.67%
Replicate 3		**Actual A_{600}**					
Acetic Acid (mM)	**A**	**B**	**C**	**Mean**	**Std. Dev.**	**% of Control**	**RSD**
0	3.946	4.312	3.664	3.974	0.3249	100%	8.18%
80	3.104	2.79	2.774	2.889	0.1861	73%	6.44%
120	2.131	2.158	2.242	2.177	0.0579	55%	2.66%
160	1.877	1.841	1.769	1.829	0.055	46%	3.01%
180	2.012	1.748	1.643	1.801	0.1901	45%	10.56%
200	1.407	1.4	1.55	1.452	0.0847	37%	5.83%
220	0.292	0.208	0.194	0.231	0.0531	6%	22.95%
240	0	0	0.006	0.002	0.0036	0%	173.21%
Replicate 4		**Actual A_{600}**					
Acetic Acid (mM)	**A**	**B**	**C**	**Mean**	**Std. Dev.**	**% of Control**	**RSD**
0	4.686	4.646	4.844	4.725	0.1047	100%	2.22%
80	3.16	2.732	3.466	3.119	0.3687	66%	11.82%
120	2.17	2.214	2.61	2.331	0.2423	49%	10.39%
160	2.206	2.324	2.343	2.291	0.0742	48%	3.24%
200	0.104	0.163	0.087	0.118	0.0395	2%	33.46%
240	0	0	0	0	0	0%	0
280	0	0	0	0	0	0%	0

*Cultures were diluted as necessary such that A_{600} readings were <0.3, the upper limit of the linear range for turbid samples in the spectrophotometer. These raw A_{600} values were then multiplied by the dilution factor to calculate actual A_{600} values, indicated here as the "actual A_{600}" values.

Table A2. S288c FPS1Δ Raw dose response data

FPS1Δ acetic acid exposure YNB-4.8 adjusted data

Replicate 1 Acetic Acid (mM)	Actual A_{600}* A	B	C	Mean	Std. Dev.	% of Control	RSD
0	4.588	5.096	5.03	4.905	0.2762	100%	5.63%
80	3.576	3.696	-	3.636	0.0849	74%	2.33%
120	2.014	2.185	-	2.1	0.1209	43%	5.76%
140	2.07	2.098	-	2.084	0.0198	42%	0.95%
160	1.804	1.267	-	1.536	0.3797	31%	24.73%
200	0.0052	0.0466	-	0.026	0.0293	1%	113.03%
220	0.0029	0.0033	-	0.003	0.0003	0%	9.12%

Replicate 2 Acetic Acid (mM)	Actual A_{600} A	B	C	Mean	Std. Dev.	% of Control	RSD
0	4.082	4.184	4.52	4.262	0.2292	100%	5.38%
80	2.82	3.36	3.454	3.211	0.3421	75%	10.65%
120	2.749	2.704	1.809	2.421	0.5302	57%	21.90%
160	0.6295	1.23	0.9275	0.929	0.3003	22%	32.32%
180	0.0615	0.0254	0.0874	0.058	0.0311	1%	53.60%
200	0.019	0.0415	0.025	0.029	0.0117	1%	40.88%
220	0.0913	0.0076	0.007	0.035	0.0485	1%	137.39%

Replicate 3 Acetic Acid (mM)	Actual A_{600} A	B	C	Mean	Std. Dev.	% of Control	RSD
0	3.294	3.03	3.244	3.189	0.1402	100%	4.40%
80	2.624	2.51	2.856	2.663	0.1763	84%	6.62%
120	2.339	1.891	1.777	2.002	0.2971	63%	14.84%
160	1.3165	1.451	1.028	1.265	0.2161	40%	17.08%
180	0.4925	1.096	0.7855	0.791	0.3018	25%	38.14%
200	0.0529	0.0446	0.047	0.048	0.0043	2%	8.87%
220	0	0	0.0018	0.001	0.001	0%	173.21%
240	0.037	0	0.0093	0.015	0.0192	0%	124.71%

Replicate 4 Acetic Acid (mM)	Actual A_{600} A	B	C	Mean	Std. Dev.	% of Control	RSD
0	3.554	4.31	4.368	4.077	0.4541	100%	11.14%
80	3.352	3.334	3.46	3.382	0.0681	83%	2.01%
120	3.398	2.614	2.542	2.851	0.4748	70%	16.65%
160	2.573	2.667	2.466	2.569	0.1006	63%	3.92%
200	0.528	0.454	0.43	0.471	0.0509	12%	10.80%
240	0	0	0	0	0	0%	0
280	0	0	0	0	0	0%	0

*Cultures were diluted as necessary such that A_{600} readings were <0.3, the upper limit of the linear range for turbid samples in the spectrophotometer. These raw A_{600} values were then multiplied by the dilution factor to calculate actual A_{600} values, indicated here as the "actual A_{600}" values.

Table A3. D5A Raw dose response data

D5A acetic acid exposure YNB-4.8 adjusted data

	Actual A_{600}*			Mean	Std. Dev.	% of Control	RSD
Acetic Acid (mM)	**A**	**B**	**C**				
0	4.968	4.726	4.946	4.880	0.1338	100%	3.88%
80	3.310	3.330	3.056	3.232	0.1527	66%	3.62%
120	3.510	2.844	2.596	2.983	0.4727	61%	9.83%
160	2.177	2.189	2.164	2.177	0.0125	45%	1.25%
200	1.654	1.554	1.515	1.574	0.0717	32%	1.71%
240	1.288	1.002	1.353	1.214	0.1867	25%	3.89%
280	0.040	0.043	0.024	0.036	0.0102	1%	0.21%

D5A FPS1Δ acetic acid exposure YNB-4.8 adjusted data

	Actual A_{600}			Mean	Std. Dev.	% of Control	RSD
Acetic Acid (mM)	**A**	**B**	**C**				
0	4.160	3.924	3.606	3.897	0.2780	100%	10.09%
80	2.540	2.862	2.872	2.758	0.1889	71%	7.00%
120	1.996	2.080	1.866	1.981	0.1078	51%	4.56%
160	1.675	1.899	1.866	1.813	0.1209	47%	4.54%
200	0.539		0.376	0.458	0.1153	12%	3.07%
240	0.000	0.000	0.000	0.000	0.0000	0%	0.00%
280	0.000	0.000	0.000	0.000	0.0000	0%	0.00%

D5A EDE1Δ acetic acid exposure YNB-4.8 adjusted data

	Actual A_{600}			Mean	Std. Dev.	% of Control	RSD
Acetic Acid (mM)	**A**	**B**	**C**				
0	5.656	5.052	5.942	5.550	0.4544	100%	11.58%
80	3.708	3.708	3.222	3.546	0.2806	64%	7.27%
120	2.474	2.246	2.576	2.432	0.1690	44%	4.71%
160	1.915	1.870	2.360	2.048	0.2708	37%	5.74%
200	1.378	1.603	1.531	1.504	0.1149	27%	3.03%
240	1.442	1.057	0.956	1.152	0.2565	21%	4.92%
280	0.098	0.108	0.093	0.100	0.0075	2%	0.20%

D5A MVB12Δ acetic acid exposure YNB-4.8 Adjusted Data

	Actual A_{600}			Mean	Std. Dev.	% of Control	RSD
Acetic Acid (mM)	**A**	**B**	**C**				
0	4.382	3.898		4.140	0.3422	100%	11.69%
80	4.030	3.582	3.952	3.855	0.2393	93%	9.63%
120	2.944	2.558	2.562	2.688	0.2217	65%	7.58%
160	1.622		1.344	1.483	0.1966	36%	5.60%
200	1.053	1.017	0.859	0.938	0.1032	23%	3.12%
240	0.040	0.045	0.035	0.040	0.0052	1%	0.15%
280	0.038	0.031	0.026	0.032	0.0058	1%	0.15%

*Cultures were diluted as necessary such that A_{600} readings were <0.3, the upper limit of the linear range for turbid samples in the spectrophotometer. These raw A_{600} values were then multiplied by the dilution factor to calculate actual A_{600} values, indicated here as the "actual A_{600}" values.

Figure A1. Replicate one dose response graph

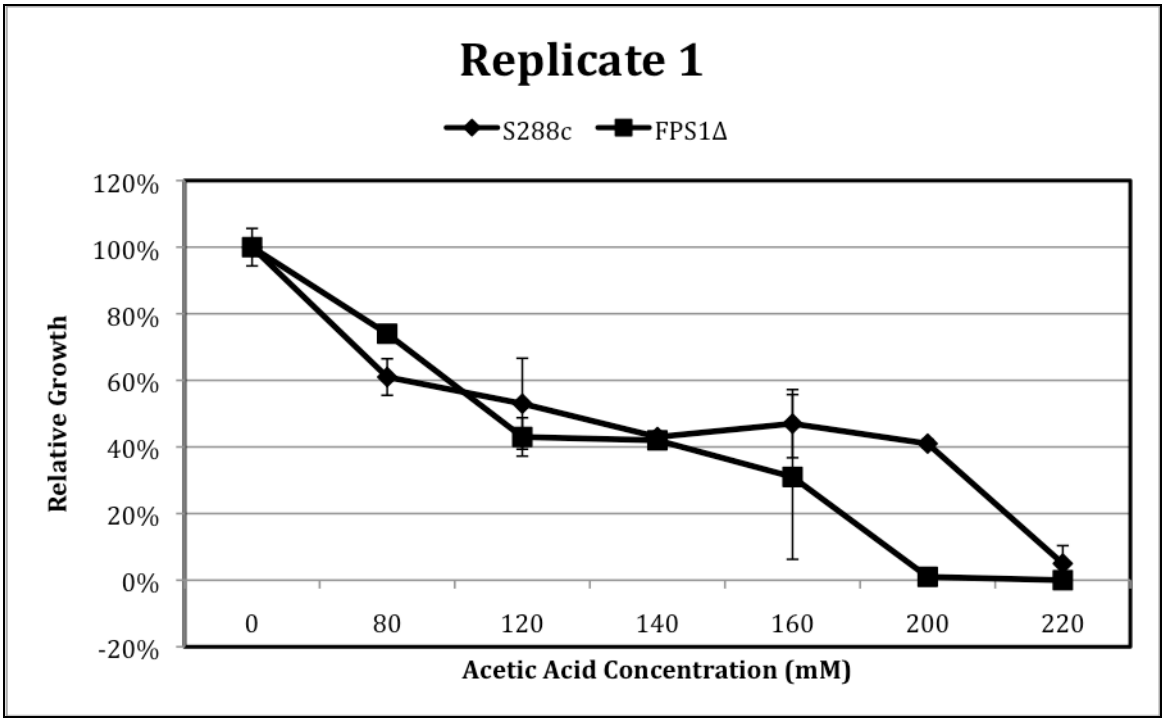

Figure A1. Mean relative growth of S288c and S288c FPS1Δ::KanMX from replicate 1. The Y-axis is relative growth which is the ratio of the A_{600} value in the presence of acetic acid to the A_{600} value in the absence of acetic acid. Error bars are relative standard deviations.

Figure A2. Replicate two dose response graph

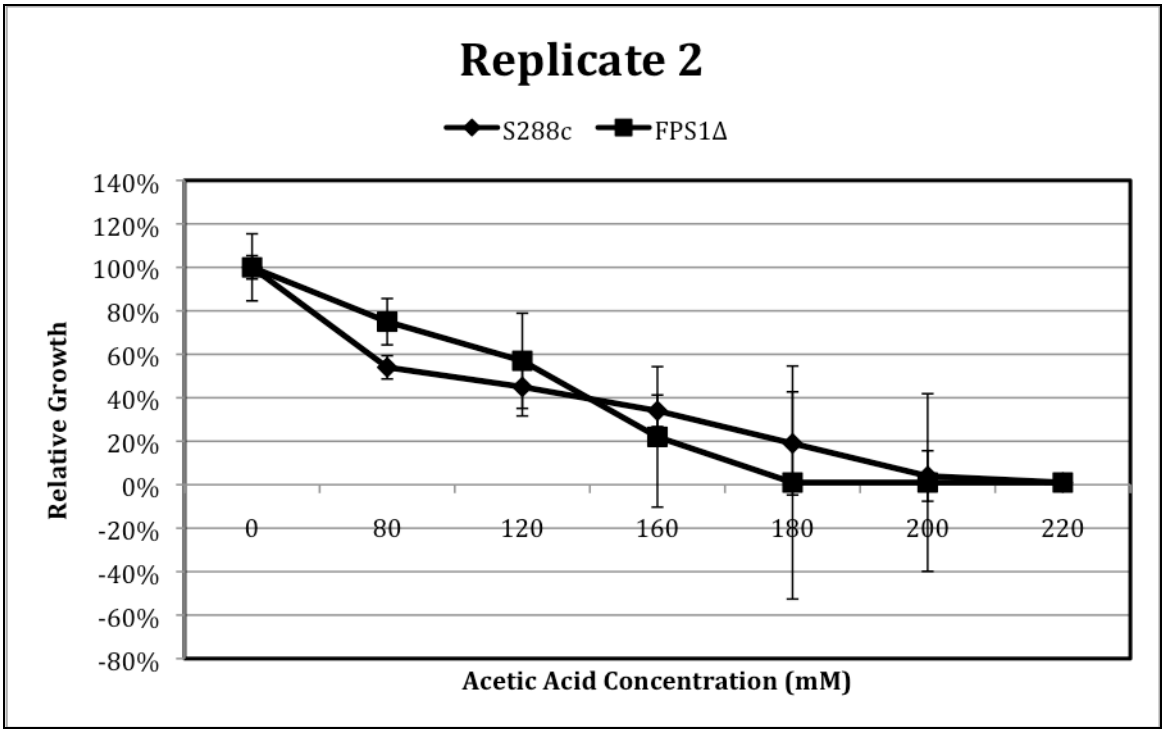

Figure A2. Mean relative growth of S288c and S288c FPS1Δ::KanMX from replicate 2. The Y-axis is relative growth which is the ratio of the A_{600} value in the presence of acetic acid to the A_{600} value in the absence of acetic acid. Error bars are relative standard deviations.

Figure A3. Replicate three dose response graph

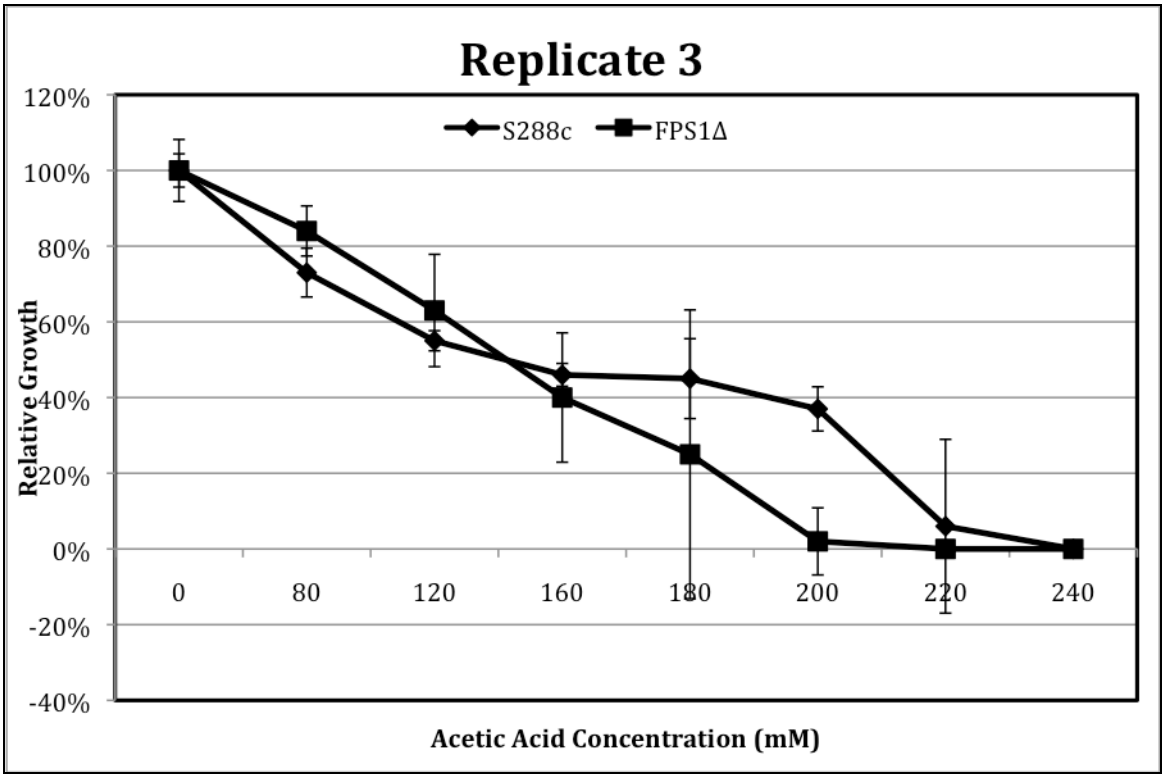

Figure A3. Mean relative growth of S288c and S288c FPS1Δ::KanMX from replicate 3. The Y-axis is relative growth which is the ratio of the A_{600} value in the presence of acetic acid to the A_{600} value in the absence of acetic acid. Error bars are relative standard deviations.

Figure A4. Replicate 4 dose response graph

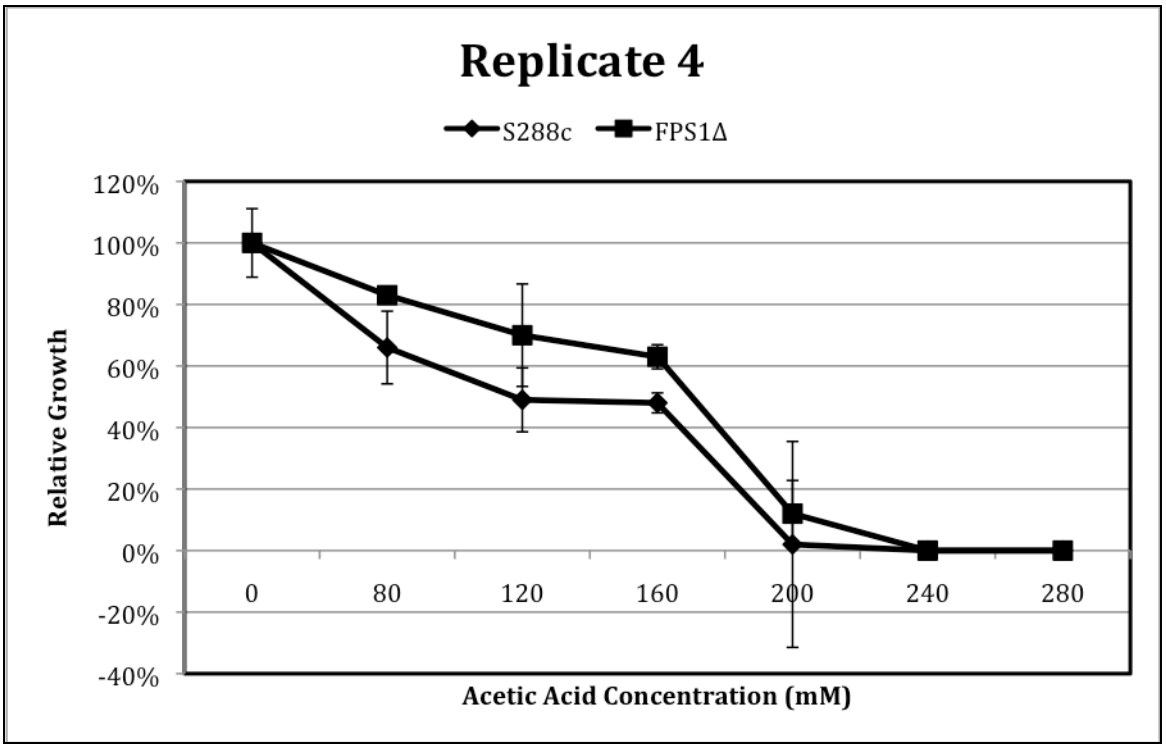

Figure A4. Mean relative growth of S288c and S288c FPS1Δ::KanMX from replicate 4. The Y-axis is relative growth which is the ratio of the A_{600} value in the presence of acetic acid to the A_{600} value in the absence of acetic acid. Error bars are relative standard deviations.